Biosensors and Bioelectronics ▮ (▮▮▮▮) ▮▮▮–▮▮▮

Contents lists available at SciVerse ScienceDirect

Biosensors and Bioelectronics

journal homepage: www.elsevier.com/locate/bios

CRP detection from serum for chip-based point-of-care testing system

Chang-Hoon Kim [a], Jae-Hyuk Ahn [a], Jee-Yeon Kim [a], Ji-Min Choi [a], Kyung-Choon Lim [b], Tae Jung Park [c], Nam Su Heo [d], Hee Gu Lee [e], Jong-Wan Kim [f], Yang-Kyu Choi [a,*]

[a] Department of Electrical Engineering, KAIST, Daejeon 305-701, Republic of Korea
[b] College of Nursing, Department of Nursing, Sungshin Women's University, Seoul 142-732, Republic of Korea
[c] Department of Chemistry, Chung-Ang University, Seoul 156-756, Republic of Korea
[d] BioProcess Engineering Research Center, KAIST, Daejeon 305-7.1, Republic of Korea
[e] Medical Genomic Research Center, Korea Research Institute of Bioscience and Biotechnology, 111 Gwahangno, Yuseong-gu, Daejeon 305-806, Republic of Korea
[f] Department of Laboratory Medicine, DanKook University, 16-5 AnSeo Dong, CheonAn 330-714, Republic of Korea

ARTICLE INFO

Article history:
Received 17 July 2012
Accepted 21 August 2012

Keywords:
C-reactive protein
CRP
Nanogap-embedded FET
FET-based biosensor
Point-of-care testing (POCT)

ABSTRACT

Most of point-of-care testing (POCT) to improve facilitates in diagnosis, treatment, and monitoring of patients. POCT technique has still remained a quantitatively and accurately detective effect. In this article, we demonstrated that real human C-reactive protein (CRP) in serum was detected for a chip-based point-of-care testing application based on a nanogap-embedded field effect transistor (FET), and the results were compared with those obtained *via* the enzyme-linked immunosorbent assay (ELISA) method. The limit of detection (LOD), determined from the standard curve, was 0.1 ng/ml, which is comparable to that of commercialized ELISAs. We evaluated that an improved detection range (0.1 ng/ml to 100 ng/ml) was achieved by comparing with commercialized ELISA. Control experiments to determine selectivity and to discern false-positive/false-negative rates were also performed. This report is the first description of the detection of CRP in human serum using a silicon-based biosensor.

1. Introduction

C-reactive protein (CRP) is one of the most important acute-phase proteins (Thompson et al., 1999). An acute-phase protein exists in the blood normally and is rapidly increased or decreased following injury, trauma, or various diseases including heart attack, infections, burns, chronic inflammation, and cancer. As many of acute-phase proteins such as serum amyloid A (SAA, Uhlar and Whitehead, 1999), mannose-binding lectin (MLB, Herpers et al., 2009), and alpha 1-antitrypsin (A1AT, Gordon et al., 1972), CRP concentration is increased upon tissue damage to enhance the inflammatory function of the leukocytes that remove the invading virus or bacteria. CRP attaches to the exogenous invading agent and induces white blood cells or other leukocytes to attack the agent. Normally, *i.e.*, no injury/disease, CRP concentration in blood is 10 mg/l, and upon injury/disease, the concentration is increased up to 1000-fold (Clyne and Olshaker, 1999). Therefore, CRP is routinely measured in the clinic to assess physical condition or surgery prognosis. In a field of clinical application, CRP is more informative than LDL-cholesterol because it provides prognostic information at all levels of calculated Framingham Risk and at all levels of the metabolic syndrome. Using widely available high-sensitivity assays, CRP levels of <1, 1 to 3, and >3 μg/ml are corresponding to normal, low-, and high-risk groups for future cardiovascular events. Evidence showed that this could cover a commonly missed scope of diagnosis by LDL-cholesterol. Thus the addition of CRP to standard cholesterol evaluation may provide a simple method to improve global risk prediction and compliance with preventive approaches (Ridker, 2003).

There are various methods to detect CRP, such as immuno assays (Highton and Hessian, 1984), visual agglutination (Senju et al., 1986), and the enzyme-linked immunosorbent assay (ELISA, Barka et al., 1985; Wu et al., 2002). However, those methods have common drawbacks, *i.e.*, requirement of large size optical equipment and signal transformation from the acquired optical data to electrical signal for data processing. Despite of those drawbacks, ELISA is the most widely used technique in the clinic because it guarantees accuracy and allows quantitative analysis of CRP concentration. Even though ELISAs offer many advantages compared to other methods, the requirement of a skilled operator and expensive as well as bulky equipment make it unsuitable for use in point-of-care testing (POCT) system, which would help one who want to check his physical condition independently at any time and place without visiting a hospital.

To use CRP as an acute-phase protein in a POCT system, a new CRP detection method is required that uses a biosensor with properties, including real-time detection with an electrical method, portability by virtue of miniaturization, and it should

* Corresponding author. Tel.: +82 42 350 3477; fax: +82 42 350 8565.
E-mail address: ykchoi@ee.kaist.ac.kr (Y.-K. Choi).

0956-5663/$ - see front matter © 2012 Elsevier B.V. All rights reserved.
http://dx.doi.org/10.1016/j.bios.2012.08.047

also be disposable and low in cost. The mainstream development of biosensors for CRP detection that satisfy these properties have focused on silicon-based biosensors, such as silicon-nanowire biosensors and ion-sensitive field effect transistor (ISFET)-based biosensors, which can be implemented on a single chip *via* commercialized silicon technology. There have been many reports of CRP detection using silicon-based biosensors (Lee et al., 2008; Kwon et al., 2011), which utilize a single-chip structure for POCT applications. However, these previous reports were presented as proof-of-concepts of the proposed biosensor using purified CRP samples. Clinical demonstration of actual serum sample tests is required for commercializing a biosensor in addition to standard curve. The results from actual serum samples should be compared with the standard curve and false-positive/false-negative rates should be noted. Moreover, we here employed an approach that uses silicon-binding proteins (SBP) (Gu et al., 2009; Sarikaya et al., 2003; Taniguchi et al., 2007), which strongly bind the SiO_2 surface with one end and fuse the immunoglobulin-binding molecule, protein A (spA) with the other end, in forms of genetically engineered fusion protein. Therefore, the efficient immobilization tool on the SiO_2 surface without any chemical surface modification was used in this study.

In this study, we detected CRPs using a simple immobilization method in a human serum sample and fit the results to a standard curve. False-positive and false-negative tests were also performed, which are indispensable for commercializing the biosensor.

2. Materials and methods

2.1. Operational principles

A device for CRP detection was fabricated using a fully conventional complementary metal oxide semiconductor (CMOS) process to guarantee small size for portability, disposability by low cost, and amenability to large-scale production which allow the application of the biosensor to POCT systems. Because the fabrication process is very common and straightforward, it was explained in supplementary information. Fig. 1a presents a schematic illustration of the fabricated device, which has a nanogap at the edge of the gate oxide in a conventional FET structure. Target molecules were introduced into the nanogap and changed the characteristics of the device. Fig. 1b is a transmission electron microscope (TEM) image of the nanogap. The nanogap was 50 nm in height and 450 nm in length with a 5 nm thick layer of regrown oxide, which were optimized in the previous report (Kim et al., 2011).

The current flow of a conventional FET device is controlled by the applied gate voltage. The electric field generated by the applied gate bias penetrates through the gate oxide and affects the carrier density of the channel area. When biomolecules are introduced into the sensing area, *i.e.*, the nanogap of the gate oxide layer, the electric field from the gate is changed accordingly, and the carrier density under the sensing area is modulated. The altered carrier density of the channel can be assessed directly by tracing the threshold voltage (V_T). The threshold voltage is one of the most important parameters in a FET because it determines the turn-on/off state of the device. The basis of the biosensor mechanism can be explained as follows: When a nanogap is formed to prepare the sensing region, the gate dielectric material between the gate and channel is changed from SiO_2 to air. The electric field from the gate is weakened because the dielectric constant of air is smaller ($k=1$) than that of SiO_2 ($k=3.9$), and thus, a higher gate voltage is required to change the carrier density, and the threshold voltage is increased. When CRP is introduced into the nanogap, two factors should be considered. The first factor is the increase in dielectric constant, because the air ($k=1$) is replaced by CRP ($k>1$). The increased dielectric constant intensifies the electric field from the gate, and thus, the threshold voltage is reduced. The second factor is the negative charges of CRP. The negative charges of CRP act like a fixed charge. The negative fixed charge between the gate and the channel weakens the electric field, thereby increasing the threshold voltage of the device. The aforementioned two factors compete in an n-channel FET when CRP is introduced into the sensing area. However, it has been reported that most of the threshold voltage change by the dielectric constant occurs during the first biomolecule immobilization step, *i.e.*, an immobilization step of the bilinker, which connects the silicon surface and the anti-CRP (Kim et al., 2008). Therefore, the negative charges of CRP bound to the anti-CRP are the predominant factors causing threshold voltage change, and thus, the threshold voltage is increased after CRP immobilization.

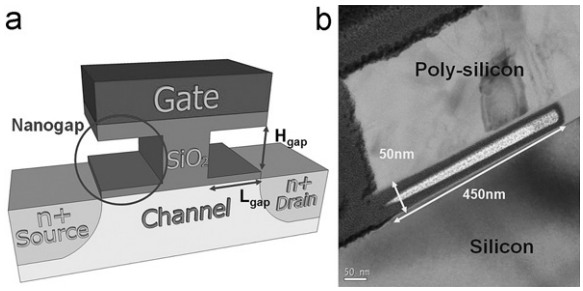

Fig. 1. (a) Schematic diagram of a nanogap-embedded field effect transistor and (b) TEM image of the nanogap. The nanogap is a sensing region and its dimension is 50 nm in height and 450 nm in length. The TEM photograph is a close-up view of the circle in (a).

2.2. Reagents

2.2.1. Reagents

Unless stated, all chemical reagents were purchased from Sigma-Aldrich (USA). All restriction enzymes were purchased from New England Biolabs (USA). Phosphate-buffered saline (PBS, pH 7.4, from BD Biosciences, USA) was used as a flow solution and a dilution buffer for the surface plasmon resonance (SPR) analysis. Distilled water (18 MΩ cm) was obtained using an ultrapure water system (Milli-Q; Millipore, USA).

2.2.2. Preparation of SBP-spA fusion proteins

Bifunctional fusion proteins were created by genetically fusing SBP and spA, allowing specific interactions between SBP and silica substrates as well as the capture of spA and antibodies. A six-histidine (6His) tag was used to allow easy purification of the fusion proteins. The DNA fragments encoding the incomplete 6His-SBP was initially obtained by PCR amplification using the primers P1 (5′-AAATATACATATGCACCATCACCACCACCACAGCCCACACCC-GCACCCACGTCACCATCACACCTTGAAAGGCGAAACAACT-3′) and P2 (5′-TCACACCCCATGGATATCGGAATTAATTCGGATCCGAATTCGAGC-TCCGTCGACAAGCTTGCG-3′), and the plasmid pET-22b(+) (Novagen, US) was used as a template. The product was then ligated into the *Nde*I and *Hin*dIII sites of pET-22b(+) to generate pET-6HSBP1. For the cloning of protein A, the primers P3 (5′-CATCCCATGGGCG-CAACACGATGAAGCTCAA-3′) and P4 (5′-TTGCT;CGAGTAGTTCGCGAC-GACGTCC-3′) were used to amplify the *spA* gene fragments encoding the protein A using a genomic DNA fragments from *Staphylococcus aureus* Mu50 (ATCC 700699D; US) as a template. The protein A PCR gene product was digested using *Nco*I and *Xho*I. The product was then ligated into the *Nco*I and *Xho*I sites of pET-6HSBP1 to generate pET-6HSBP1-spA.

For the production of the 6His-SBP-spA fusion protein, *Escherichia coli* BL21(DE3) (F^- *ompT* $hsdS_B$ (r_B^- m_B^-) *gal dcm* (DE3), Novagen) harboring pET-6HSBP-spA were cultivated in 100 ml of Luria–Bertani (LB) medium (10 g/l tryptone, 5 g/l yeast extract, 5 g/l NaCl) supplemented with ampicillin (Ap, 100 μg/ml) in a shaking incubator at 37 °C and 200 rpm. Cell growth was monitored by measuring the optical density at 600 nm (OD_{600}) using a spectrophotometer (DU®650; Beckman, US). When the cultures reached OD_{600} values of 0.4, the expression of the *T*7 promoter was induced by adding 1 mM (final concentration) of isopropyl-β-D-thiogalactopyranoside (IPTG) to the culture broth. Following the addition of IPTG, the cells were cultivated for an additional 6 h. The cells were then harvested and disrupted by sonication (Braun Ultrasonics, US) for 1 min at 20% output power. After centrifugation at 16,000 × *g* for 10 min at 4 °C, the pellet containing the soluble protein fraction with high-level expressed target fusion-protein was collected for purification of the fusion protein. Because of the 6His tags, a HisTrap™ column (GE Healthcare, UK) was used to purify the fusion protein without further purification steps. The protein concentration was determined by the Bradford assay with bovine serum albumin (BSA) as a standard.

2.2.3. Preparation of anti-CRP antibody

After the CRP gene was cloned into the pEZ vector, it was digested using the restriction enzymes *Eco*RI and *Xho*I and ligated into the *E. coli* expression vector pET-28a (Novagen) and transformed into *E. coli* BL21(DE3) to produce the recombinant CRP protein. CRP protein expression in *E. coli* was induced by adding IPTG up to a final concentration of 0.8 mM at 37 °C for 5 h. The CRP protein extraction and purification were performed according to the QIAexpression protocol (Qiagen). Briefly, the cells were lysed by a lysis buffer (50 mM · NaH_2PO_4, 300 mM · NaCl, 10 mM · imidazole, pH 8.0), and the lysates were centrifuged. After adding the cleared lysates to a Ni-NTA column (Qiagen) for purification, the column was washed with the lysis buffer, and the resin-bound His-CRP protein was eluted using an elution buffer (50 mM · NaH_2PO_4, 300 mM · NaCl, 250 mM · imidazole, pH 8.0). Production and elution of the His-CRP recombinant protein was verified by SDS-PAGE and Western blot analyses.

For generating monoclonal anti-CRP antibodies, *Balb/c* mice (5 weeks old, female) were immunized with a purified CRP protein-TiterMax (CytRx Corporation, US) mixture, and anti-CRP antibody production was examined using ELISA. After spleen cells from immunized, they were fused with myeloma *P3/NS1/1-Ag4-1* cells, and the fused-cell supernatants from selected cell lines were tested using ELISA. The selected hybridoma clones were propagated by injecting them into mice. To obtain purified mAb, the ascitic fluids were subsequently harvested and processed using protein A-Sepharose 4B chromatography.

2.3. Experiments

2.3.1. Binding properties of SBP-spA fusion proteins onto SPR chip surfaces

The binding of the SBP-spA fusion protein onto the surface of a SPR bare gold chip was characterized by SPR measurement using a BIAcore3000™ (Biacore AB, Sweden) with an automatic flow injection system. All experiments were performed in PBS at room temperature. A fresh SPR sensor chip was attached to a separate chip carrier for easy assembly in the SPR system. After the SPR chip was docked and primed, PBS was used to flush the activated surface and thereby minimize non-specific binding and any unbound sites by removing loosely bound material and dust. (3-mercaptopropyl)trimethoxysilane (Sigma-Aldrich, 50 μl of a 100 μg/ml solution) was injected onto the gold chip surface at a flow rate of 1 μl/min for 50 min using a liquid-handling micropipette in the SPR system to obtain a silane-functionalized surface. The surface was then washed and equilibrated using PBS. The SBP-spA fusion protein (50 μl of a 25 μg/ml solution) was injected onto the silane-coated SPR chip surface at a flow rate of 5 μl/min for 10 min. Before binding immunoglobulin G (IgG) onto protein A, 50 μl BSA of 100 μg/ml was injected to block non-specific binding for 10 min. The SPR responses are indicated in resonance units (RUs). One RU corresponds to approximately 1 pg/mm^2 of bound biomolecule (Stenberg et al., 1991). All SPR experiments for biomolecular binding in this study were conducted in PBS at a flow rate of 5 μl/min at room temperature, and all sensorgrams were fitted globally using BIA evaluation software (Biacore).

2.3.2. Optimal density of the SBP-spA-coated SPR biosensor for IgG binding

To examine the optimal binding density of the SBP-spA on the SPR chip, anti-mouse IgG (50 μg/ml) was injected onto the SBP-spA-coated SPR chip surface following BSA blocking. Furthermore, various anti-CRP antibody concentrations (12.5 μg/ml, 25 μg/ml, 50 μg/ml, and 100 μg/ml) were applied to the SBP-spA-covered chip surface, which was packed optimally as described above, for 10 min following blocking of non-specific binding with BSA for 10 min. The chip was then rinsed with PBS. The optimal concentration of IgG was determined by measuring the anti-CRP concentration that showed a significant change in signal relative to a PBS baseline.

2.3.3. CRP detection in a FET-based biosensor

To detect the target CRP, anti-CRP and CRP should be bound onto the sensing region. In general, several steps should be used to form the self-assembled monolayer. These steps include surface treatment, bi-linker between silicon surface and protein A treatment, protein A immobilization, and anti-CRP binding. However, these complicated steps make the experiments tedious and result in large data fluctuation. In this study, we used SBP linked to protein A to simplify the self-assembled monolayer formation procedure. SBP is an artificial protein that can be selectively bound onto a silicon surface without any bi-linker. Moreover, protein A was linked to the SBP initially, thus reducing the above tedious steps into one step.

To maximize the binding affinity of the SBP-spA onto the sensing area, the fabricated device was treated by a hot piranha solution (H_2SO_4: H_2O_2=1:1) for 10 min, which renders the sensing area hydrophilic. SBP-spA (25 μg/ml) was then dropped onto the device to immobilize the SBP-spA onto the sensing area for 15 min, followed by a 20 min incubation with anti-CRP (12.5 μg/ml). Finally, the target CRP was dropped onto the device for 20 min. Both a purified sample and an actual serum sample were employed as the target CRP.

3. Results and discussions

3.1. Process optimization

To confirm the successful immobilization of the genetically engineered fusion protein, SBP-spA, onto the SPR sensor chip, different concentrations of the protein (25 μg/ml, 50 μg/ml, 100 μg/ml and 200 μg/ml, respectively) were bound to the SPR chip for 10 min. The surface was then washed with PBS. As shown in Fig. 2, the dynamic and specific binding of SBP-spA onto the SPR chip was monitored directly in real-time. A sharp increase in SPR signal of up to 1000–1700 RU was observed upon introducing the SBP-spA solution to the chip surface, and approximately 55–80% of the SBP-spA remained on the surface even after washing with PBS, indicating that most of the fusion protein was immobilized robustly onto the chip surface. The obtained 1000 RU value implies that approximately 1 ng SBP-spA was immobilized onto a gold surface area of 1 mm^2.

Please cite this article as: Kim, C.-H., et al., Biosensors and Bioelectronics (2012), http://dx.doi.org/10.1016/j.bios.2012.08.047

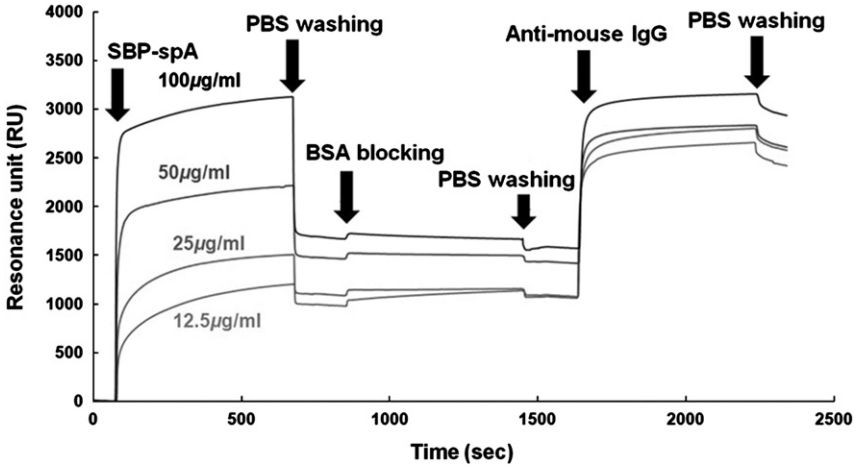

Fig. 2. SPR sensorgrams showing the specific immobilization of the SBP-spA fusion proteins at various concentrations (12.5 μg/ml, 25 μg/ml, 50 μg/ml, and 100 μg/ml, respectively) and anti-mouse IgG (50 μg/ml) onto the SPR chip, subsequently.

One RU is determined as a 0.0001° resonance angle shift and is equivalent to a mass change of 1 pg/mm^2 on the sensor surface (Lahiri et al., 1999; Subramanian et al., 2006). However, following BSA blocking and PBS washing, a SPR signal of almost 0 RU was obtained, which indicates that most of SBP-spA proteins were bound onto the SPR chip surface. After binding of SBP-spA and PBS rinsing, BSA (100 μg/ml) was allowed to flow over the SBP-spA-coated chip for 10 min to block non-specific binding. Finally, anti-mouse IgGs of 50 μg/ml were bound onto the SBP-spA-immobilized sensor chip. The binding signal of IgG to the SBP-spA layer showed approximately 1360 RU, 1500 RU, 1300 RU, and 1200 RU, respectively, from 12.5 μg/ml to 100 μg/ml of SBP-spA. SBP-spA of 25 μg/ml is an optimal condition, which makes the best packing density for the immobilization of IgG. These data showed that the SBP domain of the SBP-spA fusion protein was immobilized onto the silane-coated gold surface, and the protein A of the SBP-spA fusion protein was bound onto the IgG. Such strong binding or adsorption of SBP-fusion protein onto the SPR chip can assist in the study of various protein-protein interactions.

To investigate the optimal immobilizing density for SBP-spA and anti-CRP IgG for the detection of CRP, the optimum concentration of SBP-spA (25 μg/ml) was tested using the same concentration of IgG on the SPR chip surface. After binding of SBP-spA and PBS rinsing, BSA (100 μg/ml) was allowed to flow over the SBP-spA-coated chip for 10 min to block non-specific binding. Finally, increasing concentration of anti-CRP antibodies (12.5 μg/ml, 25 μg/ml, 50 μg/ml, and 100 μg/ml) were bound onto the SBP-spA-immobilized sensor chip. The binding signal of anti-CRP to the SBP-spA layer increased progressively from 175 RU to 2140 RU as the concentration of IgG increased from 12.5 μg/ml to 100 μg/ml (Fig. 3). However, the optimal condition determined to be 12.5 μg/ml concentration of anti-CRP. These results indicate that the optimal packing density of the bioreceptor is obtained from concentration using a 12.5 μg/ml solution. This particular anti-CRP packing density likely reduced steric hindrance and provided sufficient binding sites for the CRP antigen while avoiding loss of biological activity. Insufficiently or densely immobilized antibodies on sensing surfaces can lead to a reduced detection signal (Ko et al., 2007), and steric hindrance prevents the immobilized protein A from anchoring sufficient IgG molecules to its surface (Kolotilov et al., 2006). Thus, the optimal condition of anti-CRP was adjusted to 12.5 μg/ml concentration. These results indicate that the effective development of a specific immunoassay system may be established for CRP diagnosis using an SBP-fusion protein-immobilized chip.

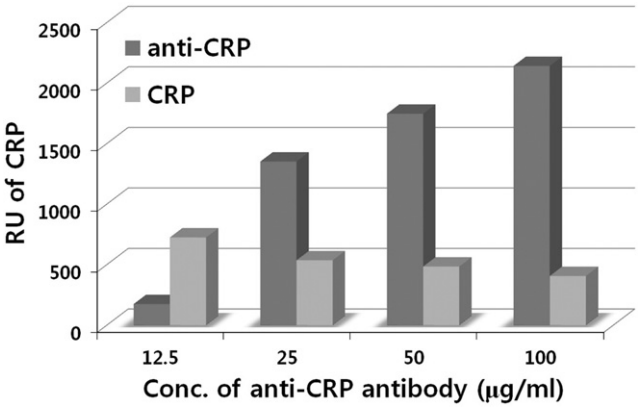

Fig. 3. The optimal concentration of anti-CRP antibody onto the SPR chip surface, showing the highest binding signal between anti-CRP antibodies and CRPs.

3.2. Characterization of the biosensor

The main purpose of this research was not to develop a new biosensor but rather to use the proposed biosensor to detect the target in actual serum samples. A standard curve which provides a reference for a quantitative analysis should be generated for accurate quantity in a purified sample of the target. The standard curve of the device was obtained using a purified sample which is calibrated by ELISA (Fig. 4). As shown in Fig. 4, the limit of detection (LOD) is 0.1 ng/ml, and the linear region, where quantitative analysis of the target CRP is possible, i.e., the detection range, ranges from 0.1 ng/ml to 100 ng/ml. It is worth noting that commercialized ELISA kits, which are well characterized and widely used in the clinic, have an LOD of 0.1 ng/ml and a detection range of 0.1 ng/ml to 5 ng/ml. Thus, the proposed device has the same LOD but a wider detection range than commercialized ELISA kits. Moreover, the ELISA kits have already been optimized. Our device is a prototype version, and the LOD may be improved with structural and experimental optimization.

3.3. Detection of CRP in serum

Results of an actual serum sample test for CRP detection are overdrawn on the standard curve in Fig. 4. Each experimental point at each concentration contains the data from 5 different devices and no device was recycled because the device will be

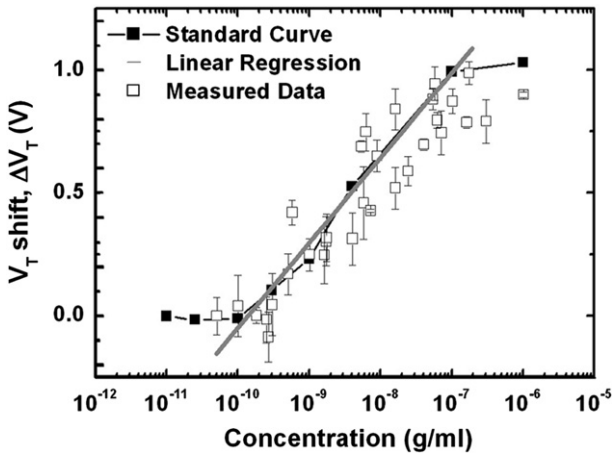

Fig. 4. The standard and linearly fitted curve of the biosensor. The equation for linear fitting is $V_T = 3.40341 \times \text{concentration} + 0.34545$. The correlation coefficient is 0.99536 and p value is less than 0.001, which implies that the standard curve can be linearly calibrated for a practical biosensor. The LOD of the device is 0.1 ng/ml, and the detection range is from 0.1 ng/ml to 100 ng/ml. The LOD is comparable to that of ELISAs, however the detection range is wider. The shift of V_T after CRP detection is overdrawn on the standard curve with standard error bar. Each experimental point at each concentration contains the data from different 5 devices.

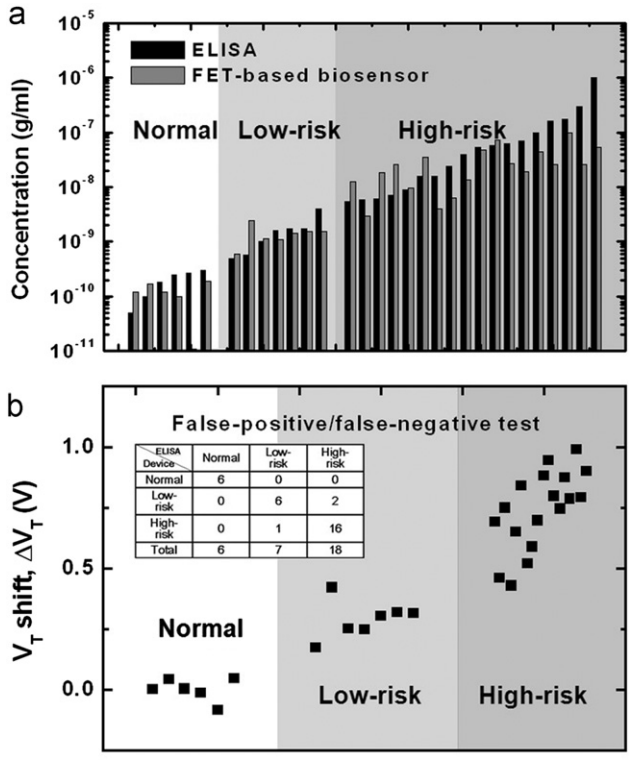

ELISA / Device	Normal	Low-risk	High-risk
Normal	6	0	0
Low-risk	0	6	2
High-risk	0	1	16
Total	6	7	18

Fig. 5. (a) A comparison of the detection results using the ELISA method, showing very similar results. (b) False-positive/false-negative tests. The normal serum sample is distinguishable from the low-risk and high-risk serum sample. However, a slight overlap between the low-risk and high-risk cases was observed. This overlap was caused primarily by data fluctuation, which can be prevented by increasing the numbers of sensing device.

applied to POCT system, which may prefer to dispose a sensor kit rather than to reuse it. The results are an average value generated from 5 different devices using one serum sample. As shown in Fig. 4, there is some variability when serum samples were tested. These variations are due to presence of undesired biomolecules in the serum. Nevertheless, the results from 31 serum samples showed a trend that correlated closely with the standard curve. The variations may be reduced by increasing the number of measuring devices.

The reliability of these results was confirmed by comparing them to those obtained *via* an ELISA. Fig. 5a presents a comparison of the measured concentration using the proposed device and an ELISA kit, respectively. The ELISA kit used in this experiment was purchased from ASSAYPRO (USA). The LOD of the ELISA kit is 0.25 ng/ml, and the detection range is from 0.25 ng/ml to 5 ng/ml. Six normal samples, seven low-risk samples, and eighteen high-risk samples were compared. As shown in Fig. 5a, although the proposed device showed a slightly smaller concentration compared to the concentration measured by the ELISA kit, the error is negligible (The p values of normal, low-risk, and high risk with the Paired t-test are 0.21321, 0.69516, and 0.1215, respectively).

3.4. Reliability test

False-positive/false-negative tests were performed, and the results are illustrated in Fig. 5b. There was no significant shift in V_T in serum from normal individuals, which implies that false-positives did not occur. Data from the high-risk cases showed sufficient V_T shift to distinguish them from the normal samples; thus false negatives did not occur, either. However, there were some overlaps between the low-risk and high-risk cases. These overlaps were caused primarily by data fluctuation, which could be prevented by increasing the number of sensing devices. The table inserted in Fig. 5b was used to calculate false-positive and false-negative rate. The calculated false-positive and false negative rate are 1/7 and 1/9, respectively. Control experiments to test

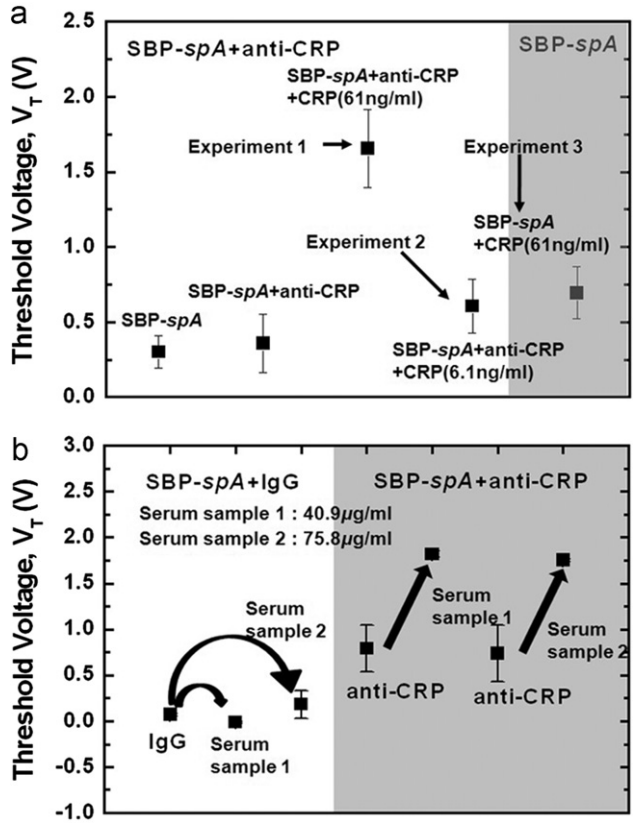

Fig. 6. (a) A specificity test for SBP-spA. The SBP-spA does not react with either CRP or any other biomolecules in the serum sample. (b) A specificity test for CRP. IgG is a control antibody for the specificity test. The target CRP did not react with IgG, *i.e.*, no V_T shift. Only anti-CRP bound specifically to CRP. The data points include 5 data obtained 5 different device for the same samples.

specificity were carried out. Initially, we checked the specificity toward SBP. A general experimental sequence is comprised of the following three steps. First, the device was treated with SBP-spA to produce a bi-linker between the silicon surface and anti-CRP. After then anti-CRP was immobilized on the SBP-spA for specific reaction with target CRP. The target CRP was then detected by antigen-antibody reactions. To assess specificity, experiment 1 used the aforementioned general sequence of CRP detection with a serum sample carrying high enough levels of CRP (61 ng/ml) thereby it can lead to changing the device characteristics significantly, and experiment 2 used a 10-fold diluted sample of the serum used in experiment 1. In experiment 3, anti-CRP immobilization was omitted, and the target serum was the same as used in experiment 1. The results are shown in Fig. 6a. Experiments 1 and 2 confirmed the proper operation of the device. Experiments 1 and 3, confirmed that CRP and other molecules in the serum sample did not affect the device because in experiment 3, we did not detect a significant threshold voltage shift, whereas in experiment 1, we detected a voltage shift exceeding 1 V. These data indicate that the SBP-spA did not affect the operation of the biosensor, and only anti-CRP reacted selectively with target CRP. A second control experiment was performed to check the specificity of the target CRP. To assess the specificity of the target CRP, whole IgG of rabbit was used. Following SBP-spA immobilization, the whole IgG and anti-CRP were bound separately onto the SBP-spA as a receptor of target CRP. As shown in Fig. 6b, V_T was not changed when the target CRP reacted with the whole IgG, whereas more than 1 V of V_T was detected after target CRP treatment on anti-CRP. The concentration of the target CRP used in this experiment was sufficiently high, *i.e.*, in the low μg/ml range, which corresponds to the concentration in the saturation region of the standard curve, to enable a clear distinction of the V_T shift. These data prove that the target CRP reacted only with anti-CRP. Thus, it is concluded that the V_T shift in the biosensor occurred due to the specific binding of anti-CRP and CRP and not by non-specific binding to other biomolecules in the serum sample or bi-linker (SBP-spA).

4. Conclusions

In this study, CRP in human serum samples was detected using a FET-based biosensor for application in POCT. First, this process is very simple, requiring merely one-step to immobilize the recognition element onto the chip surface without surface chemical modification; strong affinity between the SBP and the surface of silicon oxide guarantees stability preventing possible leakage of sensing proteins; binding of SBP onto the surface of silicon oxide also might help to expose sensing molecules outward to react with their targets by arrangement for correct orientation of bioreceptor. Furthermore, the obtained standard curve displayed a comparable LOD and improved detection range relative to commercialized ELISA kits. We confirmed possible application in serum samples by false-positive/false-negative and specificity tests. Although the number of target serum samples was too small to judge the reliability of the biosensor, we suggest that CRP in serum can be detected using a FET-based biosensor. In conclusion, these data indicate that this novel detection method potentiates new paradigm of CRP detection in human serum using a silicon-based biosensor.

Acknowledgements

This work was supported by the National Research Foundation of Korea (NRF, 2011-0020487) and the National Research and Development Program (NRDP, 2011-0002182) for the development of biomedical function monitoring biosensors and the Technology Innovation Program through the Korea Innovation Cluster Foundation funded by the Ministry of Knowledge Economy (A2010D-D013) and was sponsored by the Korea Ministry of Education, Science and Technology (MEST).

Appendix A. Supporting information

Supplementary data associated with this article can be found in the online version at http://dx.doi.org/10.1016/j.bios.2012.08.047.

References

Barka, N., Tomasi, J.-P., Stadtsbaeder, S., 1985. Journal of Immunological Methods 82, 57–63.
Clyne, B., Olshaker, J.S., 1999. The Journal of Emergency Medicine 17, 1019–1025.
Gordon, H.W., Dixon, J., Rogers, J.C., Mittman, C., Lieberman, J., 1972. Human Pathology 3, 361–370.
Gu, B., Park, T.J., Ahn, J.-H., Huang, X.-J., Lee, S.Y., Choi, Y.-K., 2009. Small 5, 2407–2412.
Herpers, B.L., Endeman, H., Jong, B.A.W., Jongh, B.M., Grutters, J.C., Biesma, D.H., Velzen-Blad, H., 2009. Clinical & Experimental Immunology 156, 488–494.
Highton, J., Hessian, P., 1984. Journal of Immunological Methods 68, 185–192.
Kim, C.-H., Jung, C., Park, H.G., Choi, Y.-K., 2008. Biochip 2, 127–134.
Kim, C.-H., Jung, C., Lee, K.-B., Park, H.G., Choi, Y.-K., 2011. Nanotechnology 22, 135502.
Ko, S., Kim, B., Jo, S.-S., Oh, S.Y., Park, J.-K., 2007. Biosensors and Bioelectronics 23, 51–59.
Kolotilov, S.V., Boltovets, P.N., Snopok, B.A., Pavlishchuk, V.V., 2006. Theoretical and Experimental Chemistry 42, 211–216.
Kwon, S.M., Kang, G.B., Kim, Y.T., Kim, Y.H., Ju, B.K., 2011. Journal of Nanoscience and Nanotechnology 11, 1511–1514.
Lahiri, J., Isaacs, L., Tien, J., Whitesides, G.M., 1999. Analytical Chemistry 71, 777–790.
Lee, M.-H., Lee, K.-N., Jung, S.-W., Kim, W.-H., Shin, K.-S., Seong, W.-K., 2008. International Journal of Nanomedicine 3, 117–124.
Ridker, P.M., 2003. Journal of the American Heart Association 107, 363–369.
Sarikaya, M., Tamerler, C., Jen, A.K., Schulten, K., Baneyx, F., 2003. Nature Materials 2, 577–585.
Senju, O., Takaqi, Y., Uzawa, R., Iwasaki, Y., Suzuki, T., Gomi, K., Ishii, T., 1986. Journal of Clinical & Laboratory Immunology 19, 99–103.
Stenberg, E., Persson, B., Urbaniczky, C., 1991. Journal of Colloid and Interface Science 143, 513–526.
Subramanian, A., Irudayaraj, J., Ryan, T., 2006. Sensors and Actuators B: Chemical 114, 192–198.
Taniguchi, K., Nomura, K., Hata, Y., Nishimura, T., Asami, Y., Kuroda, A., 2007. Biotechnology and Bioengineering 96, 1023–1029.
Thompson, D., Pepys, M.B., Wood, S.P., 1999. Structure 7, 169–177.
Uhlar, C.M., Whitehead, A.S., 1999. European Journal of Biochemistry 265, 501–523.
Wu, T.-L., Tsao, K.-C., Chang, C.P.-Y., Li, C.-N., Sun, C.-F., Wu, J.T., 2002. Clinica Chimica Acta 322, 163–168.